

SLAC-PUB-4945

May 1990

(A)

OXIDE OVERLAYERS AND THE SUPERCONDUCTING RF  
PROPERTIES OF YTTRIUM-PROCESSED HIGH-PURITY NB \*

F. L. PALMER<sup>+</sup>

*Newman Laboratory of Nuclear Studies  
Cornell University, Ithaca, N. Y. 14853*

and

R. E. KIRBY, F. K. KING, AND EDWARD L. GARWIN

*Stanford Linear Accelerator Center  
Stanford University, Stanford, California 94309*

*Submitted to Journal of Applied Physics*

---

\* Work supported by the Department of Energy, contract number DE-AC03-76SF00515 and National Science Foundation Cooperative Agreement PHY84-12263.

- ABSTRACT

Superconducting rf surface resistance measurements were made on oxidized Nb cavities that been warmed for a few minutes to temperatures between 250 and 300°C. Warmed oxide layers were further studied using x-ray photoelectron spectroscopy, Auger electron spectroscopy and secondary electron emission yield measurements. Warming usually reduced the temperature-dependent (BCS) part of the surface resistance by 10-20% while, for warming temperatures near 300°C, the low-temperature residual surface resistance increased by as much as 70 nano-ohms. Surface spectroscopy measurements showed that, at temperatures between 200 and 250°C, the oxide layer was chemically altered but remained surface-segregated; between 250 and 300°C, however, surface oxygen dissolved into the Nb bulk. Changes in the BCS resistance were consistent with a model based on a shortening of the electron mean free path by oxygen that had diffused into the Nb metal and based on the theoretical dependence of BCS resistance on electron mean free path. No specific cause for the increased residual resistance could be positively identified, although oxygen-induced surface roughening is a possibility.

## INTRODUCTION

Nb superconducting radio-frequency (rf) cavities are critical to the operation of the next generation of particle accelerators. Power losses in these structures are directly related to the rf surface resistance. Since Nb surfaces are almost always covered by an oxide layer, the influence of oxides on surface resistance is of interest. Recent observations<sup>[1]</sup> have shown that the surface resistance is substantially altered on Nb cavities where the oxide layer has been warmed to  $\approx 300^\circ\text{C}$  for a few minutes. In particular, the residual resistance, which always dominates the losses at sufficiently low temperatures, can increase by as much as 70 nano-ohms. In this paper, we have used x-ray photoelectron spectroscopy (XPS), Auger electron spectroscopy (AES) and secondary electron emission yield measurements, as well as superconducting rf measurements to describe the evolution of these oxide layers as they are heated. While oxides such as metallic NbO or non-stoichiometric Nb<sub>2</sub>O<sub>5</sub> are often proposed as causes of residual resistance, we found no evidence linking any oxide to the increase in residual resistance.

## EXPERIMENTS

XPS, AES, and secondary yield measurements were done on 0.05 cm-thick, polycrystalline Nb samples taken from the same material used to manufacture cavities for the present study and for reference 1. The raw materials, which came from several sources, were yttrium processed to reduce substantially the bulk oxygen content. The samples, which had residual resistivity ratios (RRR) between 100 and 150, were ultra-high-vacuum (UHV) fired in an rf furnace at  $1200^\circ\text{C}$  for 20 minutes and then raised to  $1400^\circ\text{C}$  for one minute. They were then transferred

*in vacuo* to the chamber<sup>[2]</sup> where the surface analytical spectrometers were located. Samples could be warmed in the spectrometer chamber to 350°C or more by electron bombardment of the back of the sample. Firing temperatures were monitored by visible (0.65 micron) pyrometry, while temperatures near 300°C were monitored with an infrared (1.6-2.7 microns) pyrometer. An adjoining chamber was used to expose the samples to 0.1 torr of dry oxygen for two hours. Two types of surface studies were performed. The first experiments followed the procedures of reference 1 as closely as possible. Measurements were made at room temperature after the samples were UHV fired, exposed to oxygen, and warmed to 300°C. The second set of measurements was made on samples as they were warmed from room temperature to 350°C, after they had been fired and exposed to oxygen.

For comparison with these later measurements, superconducting rf measurements were made on a fired and oxidized cavity that was warmed to successively higher temperatures with cryotests following each warming. The procedure for firing the cavities is described elsewhere<sup>[3]</sup>. Cavities were warmed by placing an aluminum can over the top of the cavity while the cavity interior remained connected to an ion pump. Heater coils were wrapped around the can and around the pumping tube of the cavity. The temperature was monitored by thermocouples placed on the top and the bottom of the cavity. These thermocouples usually agreed to within 15°C.

## RESULTS

### Surface Analysis:

The principal observation from the first part of this study was that the sur-

face analytical measurements-made after firing, exposure to oxygen, and warming to 300°C were similar to measurements made immediately after firing. This was unexpected because the two surface preparations yield very different surface resistances<sup>[1]</sup>. The fired Nb was covered with less than one half monolayer of oxygen, which was probably due to a combination of precipitation from the bulk during cooldown<sup>[4]</sup>, and contamination during *in vacuo* transfer to the spectrometer chamber. After exposure to oxygen, XPS measurements showed a 1.3 nm thick layer of Nb<sub>2</sub>O<sub>5</sub>. The warming to 300°C drove most of this oxygen into the metal leaving roughly 1.5 times the coverage before oxidation. It was not possible to associate any particular stoichiometry with this sub-monolayer coverage.

AES detected both S and P contamination on some, but not all, of the samples; however, we found no evidence that their presence affected the rf or XPS results. The total secondary electron yield was not significantly affected by oxidation or warming. It remained between 1 and 1.2 over the range of incident primary electron energies from 100 to 1400 eV.

In the second part of this study, the temperature dependence of these processes was examined by monitoring the XPS spectrum while a piece of oxygen-exposed Nb was slowly warmed to 350°C. The temperature as a function of time for these measurements is shown in Figure 1. The time during which each spectrum was made is indicated with a solid line, and identified with a letter from A to D. Figure 2 shows the Nb 3d and the O 1s core level lines from each of these spectra. The signal for pure Nb metal, which consists of the two main spin-orbit-split peaks at binding energies of 202.0 and 204.8 eV, will be chemically shifted by oxidation in proportion to the valence of the Nb at a rate of about 1eV/oxidation number<sup>[5]</sup>.

The two small peaks in curve A are due to  $\text{Nb}_2\text{O}_5$  (valence  $\text{Nb}^{5+}$ ). The XPS curve-fitting procedures used in this work have been described previously<sup>[6,7]</sup>.

As the temperature approaches  $250^\circ\text{C}$  (Fig. 2B), the  $\text{Nb}_2\text{O}_5$  intensity drops; however, the Nb metal peaks, as well as the oxygen peak at 531 eV, remain at about the same height indicating that almost all the oxygen remains within the  $\approx 2\text{--}3$  nm surface layer from which the photoelectrons can escape. Seven minutes later (Fig. 2C), and 40 degrees warmer, most of the oxygen has left the surface and diffused farther into the bulk. Above  $300^\circ\text{C}$  (Fig. 2D), the Nb XPS spectrum changes slightly as the remaining traces of oxygen continue to diffuse into the bulk. After cooldown back to room temperature, the spectrum (not shown) is similar to Figure 2D except for a small further oxygen diffusion into the bulk during the cooldown period.

#### Superconducting RF Measurements:

The low temperature ( $T < T_c/2$ ) rf surface resistance of Nb can be written as the sum of two terms:

$$R(T) = R_{BCS}(T) + R_{RES}$$

where  $R_{RES}$  is a sample-dependent empirical constant, and  $R_{BCS}$  has the temperature dependence predicted by the BCS theory. Wilson<sup>[8]</sup> has shown that the Pippard limit formula,

$$R_{BCS}(T) = \frac{B}{T} \log \left( \frac{46T}{f} \right) \exp \left( -\Delta_o \frac{G(T)}{T} \right)$$

$$\text{where } G(T) = 1 - 0.82T \exp \left( -\frac{\Delta_o}{T} \right)$$

gives almost the same temperature dependence as the more detailed numerical calculations<sup>[9,10]</sup> except that the prefactor  $B$ , which depends on the frequency and mean free-path, must be included. Here  $\Delta_0$  is the zero temperature energy gap in kelvins,  $f$  is the frequency in GHz, and the function  $G(T)$  gives the temperature dependence of the gap. (The simple formula,  $R_{BCS} = (B/T) \exp(-\Delta_0/T)$  fits almost as well for  $T < 3.5\text{K}$ , but it gives a gap value that is  $\approx 0.9$  degrees too high at  $f = 8.6$  GHz.)

A series of cryogenic measurements was done for comparison with the surface studies done on gradually warmed Nb (Figure 2). Measurements were made on an 8.6 GHz "elliptical"<sup>[11]</sup> Nb cavity that had a RRR of 180. The cavity was first UHV fired at 1200°C for 20 minutes followed by 1400°C for 1 minute. Then it was moved to a cryostat and tested without exposure to air. After this test, the cavity received a single two-hour exposure to 0.1 torr of oxygen. It was then evacuated and warmed to three successively higher temperatures for 5 minutes at each temperature, with cryotests following each temperature increase.

Two sets of surface resistance measurements were made after each warming. The first set was done with the ambient magnetic field screened to  $< 2$  mG. The cavity was then warmed to above the transition temperature, a 120 mG field was applied, and the cavity was cooled and retested.

The results are shown in Figure 3(a-c). Figures 3(a) and 3(b) show the BCS resistance at 2K and the residual resistance after firing, and after oxidation and warming to three successively higher temperatures. Comparison with Figure 2 shows that the highest residual resistance was measured after warming the cavity to just above the temperature at which the  $\text{Nb}_2\text{O}_5$  oxide layer had dissolved into

the bulk. The detailed behavior with temperature is treated in the Discussion section under Residual Resistance. Figure 3(c) shows the increase in residual resistance caused by the application of a 120 *mG* magnetic field following these same treatments. The energy gap had a constant value of  $17 \pm 0.2$  K throughout this study, so the variations in the BCS resistance are variations in the prefactor B.

## DISCUSSION

### Mean Free Path Effect:

Dissolved oxygen can alter the BCS resistance of Nb by shortening the electron mean free path,  $\ell$ . Figure 4 shows the dependence of  $R_{BCS}$  on RRR at 2K, as predicted by Halbritter's program<sup>[10]</sup>. We have used Halbritter's material parameters for Nb, with the estimate,  $\ell \approx (RRR) \times (2 \text{ nm})$ . In the absence of other impurities, the RRR is related to the oxygen concentration,  $c$  (in atomic %), by  $RRR = 4.5/c$ <sup>[12]</sup>.

Our subsequent analysis is particularly dependent on the existence of a minimum in surface resistance near  $RRR = 15$  ( $c = 0.3\%$ ). Although Halbritter's program has been shown to agree very well with experiment for certain ranges of input parameter values<sup>[8]</sup>, the program is very complicated and it is derived from a single gap Green's function calculation<sup>[13]</sup> that necessarily contains many approximations. Furthermore, no experimental study of the mean free-path dependence of surface resistance has been done that covers the RRR range of interest here. Confidence may be gained from the observation that the general features of Figure 4 can be understood in terms of a simple two fluid model in which the minimum surface resistance appears at the onset of the anomalous skin effect.

The expression for the power loss per unit volume in an ordinary conductor is  $\sigma E^2 = E^2 \cdot (ne^2\tau/m)$ , where  $E$  is the electric field,  $e$  and  $m$  are the electron charge and mass, and the relaxation time is related to the mean free-path by

$$\tau = \frac{\ell}{v_f} \quad . \quad (1)$$

In a superconductor,  $n$  is replaced by the density of “normal” electrons, since the superconducting electrons exhibit no losses. If  $\ell$  is smaller than both the coherence length and the penetration depth,  $\lambda$ , then the conductivity will be local with both the supercurrent and the normal current proportional to  $\ell$ <sup>[14]</sup>. Consequently, the surface resistance is proportional to  $\ell^{-1/2}$ , as in the case of a normal metal. If, on the other hand,  $T < T_c/2$  and  $\ell$  is much greater than the coherence length, then the conduction is dominated by the supercurrent that is now essentially independent of  $\ell$ . The electric field pattern in the metal is therefore independent of  $\ell$ , making the superconductor similar to a dielectric where the fields are determined by the displacement current and the losses are proportional to the “normal” conductivity. However, since the coherence length and  $\lambda$  are similar for Nb, the normal conductivity has become non-local. Electrons which are not traveling parallel to the surface may exit the penetration layer and stop gaining energy before they travel the full distance,  $\ell$ . Therefore, the mean free-path in Equation 1 is replaced by

$$L_{EFF} = \frac{1}{4\pi} \int L(\theta) d\Omega$$

where  $\theta$  is the direction of travel with respect to the normal,  $d\Omega = 2\pi \sin \theta d\theta$ , and  $L(\theta)$  is the distance that the electron travels within the penetration layer. For electrons traveling almost parallel to the surface (such that  $|\theta - \frac{\pi}{2}| < \frac{\lambda}{\ell}$ ),  $L(\theta) \approx \ell$ ;

but the remaining electrons usually exit the surface layer without any collisions so that  $L(\theta) \simeq \frac{\lambda}{\cos \theta}$ . The surface resistance is therefore proportional to

$$L_{EFF} = \int_{\frac{\pi}{2} - \frac{\lambda}{\ell}}^{\frac{\pi}{2}} \ell \sin \theta d\theta + \lambda \int_0^{\frac{\pi}{2} - \frac{\lambda}{\ell}} \tan \theta d\theta = \lambda \left( 1 + \log \frac{\ell}{\lambda} \right).$$

The surface resistance thus increases logarithmically with mean free-path until finally  $\ell$  is so long that the collision time is longer than the rf period, at which point further increases in  $\ell$  will have little effect and the surface resistance is essentially constant. This leveling occurs at greater than  $RRR = 500$  for the frequency (8.6 GHz) used in Figure 4.

#### Oxygen Diffusion:

The sensitive temperature dependence of both the XPS and rf data near 300°C makes it difficult to establish connections between these two types of measurements; however, a tentative description of the dissolution of the oxide layer can be made based on these results and on the diffusion rate of oxygen in Nb.

Dissolved oxygen moves through Nb metal according to the diffusion equation,

$$\frac{\partial c}{\partial t} = D \frac{\partial^2 c}{\partial z^2}$$

where  $c$  is the oxygen concentration,  $z$  is the distance from the surface, and  $D$  is the diffusion constant, which depends only on the kelvin temperature<sup>[15]</sup>,

$$D = 0.02 \exp \left( \frac{-13500}{T} \right) \frac{cm^2}{sec}$$

A particularly useful solution to the diffusion equation is

$$c = \frac{A}{\delta\sqrt{\pi}} \exp\left(\frac{-z^2}{4\delta^2}\right) \quad (2)$$

where  $\delta^2$  is the time integral of the diffusion constant,  $\int D dt$ , and  $A$  is the total amount of oxygen per unit area,  $\int_0^\infty c dz$ . Since the concentration gradient is zero at the surface ( $z = 0$ ), this solution shows oxygen diffusing into the metal from near the surface without any oxygen entering or leaving the metal.

Figure 5 shows this solution to the diffusion equation for Nb that has been warmed to successively higher temperatures for 5 minutes at each temperature. Although these warmings are cumulative, the diffusion rate increases so quickly with temperature that most of the diffusion has always occurred at the most recent temperature. The concentration plotted is the ratio of the density of oxygen atoms in solution to the density of Nb atoms in the pure metal. (This dimensionless concentration equals one if 54 atoms of oxygen per cubic nm are present.) Since the observed 1.3 nm layer of  $\text{Nb}_2\text{O}_5$  contains approximately 66 atoms/nm<sup>2</sup> of oxygen, "A" was set to  $66 \text{ nm}^{-2}/54 \text{ nm}^{-3} = 1.2 \text{ nm}$ . This diffusion model ignores many properties of the stoichiometric oxide(s) found near the surface, but the original layer may be crudely approximated by setting  $\delta$  equal to 0.5 nm at  $t = 0$  so that most of the oxygen is initially within 1.5 nm of the surface.

After five minutes at 150°C, the diffusion model predicts that the oxygen will be spread out over a region at least 10 nm thick, but the XPS measurements (Figure 2) show that this is not the case. Most of the oxygen remains within 2 nm of the surface with its valence and that of the Nb essentially unchanged from that

of the room temperature oxidized surface. This suggests that the interface between the metal and the oxide is fairly sharp. Any oxygen that escapes into the metal can diffuse rapidly away from the surface, leaving relatively pure metal next to the oxide.

When the oxide finally decomposes at around 250°C, the oxygen quickly spreads out into a layer that is, according to the diffusion calculations, on the order of 100 nm thick. Since the magnetic penetration depth is between 40 and 80 nm, the surface resistance should depend on the properties of this layer. The oxygen concentration throughout the penetration layer rises as the oxide decomposes, reaches a maximum around 300°C, and then declines at higher temperatures as the oxygen diffuses farther into the bulk.

The curve through Figure 3(a) shows a simple calculation of the BCS resistance of oxidized Nb after warming to the indicated temperature for 5 minutes. The fraction,  $f$ , of the oxide layer that dissolves into the bulk at a given temperature is assumed to be given by the Fermi-type function

$$f = \frac{1}{1 + \exp[(540K - T)/15]}$$

that is in reasonable agreement with the XPS O 1s area measurements. The quantity,  $A$ , in Equation 2 is replaced by  $A_0 f$ , where  $A_0$  corresponds to 1.3 nm of  $\text{Nb}_2\text{O}_5$ . The concentration near the surface is then given by Equation 2 (with  $z = 0$ ) and the surface resistance is taken from Figure 3. A time of 200 seconds is used in Equation 2 to allow 100 seconds for the oxides to dissolve. The calculated BCS resistance exhibits two minima after warming to 250°C and 350°C. These probably correspond to bulk oxygen concentrations of around 0.1 percent. Between

these two temperatures, the oxygen concentration may rise to several tenths of a percent, causing a local maximum in  $R_{BCS}$ . At 350°C, the calculated RRR near the surface is about 35, which agrees well with the experimental value determined by measuring the normal  $Q$  of the cavity (this point is marked with an "x" on Figure 4). The  $R_{BCS}$  experimental data shows a peak at slightly above the temperature of the 275° maximum in the calculation, as would be expected, considering the activated nature of the diffusion, i.e., the surface oxygen supply is dependant on decomposition of the pentoxide.

#### Residual Resistance:

Increases in residual resistance (Figure 3b) have been previously postulated<sup>[16]</sup> as due to the formation of conducting NbO or defective Nb<sub>2</sub>O<sub>5</sub> oxides in the penetration layer. However, decomposition of our XPS spectra (Figure 2) does not support this speculation. Conventional models of the oxidation of Nb to Nb<sub>2</sub>O<sub>5</sub> include the existence of a graded layer of NbO and NbO<sub>2</sub> between the metal and pentoxide, typically produced by water oxidation but also indirectly identified as present in one UHV oxygen-oxidation study<sup>[17]</sup>. However, that graded layer does not appear to exist here (or is too thin to be detectable) for the thin oxide produced at room temperature with dry oxygen on very pure Nb. Valencies identified in the XPS spectra presented here include Nb<sup>0</sup> (metal), Nb<sup>1+</sup>, Nb<sup>5+</sup> (pentoxide) and O<sup>2-</sup> (oxide), but not Nb<sup>2+</sup>(NbO) or Nb<sup>4+</sup>(NbO<sub>2</sub>).

The oxidized room temperature curvefit spectrum, Figure 2A, is presented, with components, in Figure 6. No new spectral components, beyond those present in Figure 6, are necessary to obtain good fits of Figures 2 A-D. Note that peaks

appear in pairs, Nb  $3d_{3/2}$  and Nb  $3d_{5/2}$ , due to spin-orbit splitting. Using fired Nb 3d metal peaks (to account properly for the asymmetrical Lorentzian lineshape) in these fits for the Nb<sup>0</sup> valence components shows that the bulk of the remaining broadening of the spin-split metal peaks' intensity appears at locations (peaks 5 and 6 in Figure 6) having an energy approximately 1 eV higher than the metal peaks. If this is due to a chemical shift, it corresponds to Nb<sup>1+</sup> valence. Note that NbO (Nb<sup>2+</sup>) would occupy a binding energy site one full eV higher than this, where there is little additional intensity above the background. NbO<sub>2</sub> or valence-defective Nb<sub>2</sub>O<sub>5</sub> would produce peak components of valence 4+ to 5+ but they also do not appear as products of the curvefits of Figure 2. As the oxidized Nb surface is warmed, the intensity of the pentoxide (Nb<sup>5+</sup>) components drops to zero by Figure 2C, while that of the Nb<sup>1+</sup> peak components doubles by Figure 2D and remains unchanged after cooldown. Subsequent firing to 1400°C removes the Nb<sup>1+</sup> peak components and restores the original clean surface spectrum.

Many workers<sup>[16]</sup> studying oxidized Nb by both bulk and surface methods have observed the presence of lower- and sub-oxides and, in two cases<sup>[18,19]</sup>, a peak has appeared at 1+ valence (but was mis-identified); however, it was accompanied by peaks with valencies 2+ and 4+. Whether the 1+ peak of Figure 6 can be unambiguously associated with an oxide or another cause, and whether it is connected to the increase in the residual resistance remains to be determined. A few speculative possibilities:

- 1) The 1+ peak is due to the actual presence of Nb<sub>2</sub>O. This possibility cannot be discounted but several points work against it. First, the 1+ peak grows as the oxygen intensity drops, and remains intense after warming is complete and the

oxygen concentration has dropped back to low level. Second, no stoichiometric (valence 4+ or 2+) oxides form as the pentoxide decomposes. This supports the contention that oxygen from the pentoxide dissolves directly into the bulk upon heating, as discussed in the "Oxygen Diffusion" section above, or that the oxygen is possibly involved in another process (discussed below) that is not oxide formation, prior to dissolving into the bulk.

2) There is a localized bulk distortion of the lattice by the dissolving oxygen that causes the increased residual resistance. The oxygen concentration within one micron of the Nb surface reaches a maximum of a few tenths of a per cent after warming to roughly the same temperature that corresponds to the peak residual resistance. In addition, these high bulk concentrations may be unstable against the formation of NbO as the Nb cools<sup>[20]</sup>. This accounts for the increase in residual resistance but probably not the 1+ peak that is present following room temperature oxidation where the bulk diffusion is negligible.

3) The 1+ peak is a result of a surface structural rearrangement. Since the dry oxidation of Nb is about  $10^4$  times less efficient than wet<sup>[16]</sup>, surface dynamics favor an oxygen-catalyzed structural mass rearrangement toward lowering the surface free energy<sup>[21]</sup>, such as facet formation. Without the presence of sub-oxide building blocks, the direct formation of pentoxide is a very low probability process involving considerable atomic motion. That mass movement may lead to the formation of other structures involving the surface self-diffusion of Nb. Oxygen is the catalyst that lowers the surface diffusion barrier for this movement.

— Nb facet formation under these experimental conditions is possible. They have been observed by low energy electron diffraction (LEED) to form on the oxidized

(100) and (110) crystal faces of Nb at low temperatures, are catalyzed by oxygen and do not break up until high temperature (typically above 1000°C)<sup>[4,22]</sup>. Studies conducted on the oxidation of Ni(210), revealed the formation of facets below room temperature<sup>[23]</sup>, so extensive facet formation on Nb at a few hundred °C does not seem out of the question.

Surface-structural effects can and have been observed in XPS spectra, for example, structure-induced broadening of XPS peaks has been identified in sputter-damaged TiO<sub>2</sub> layers that exhibited vacancy-caused broadening<sup>[24]</sup> of Ti core level peaks. In another case, structural relaxation at the surface, e.g., because of chemisorption, can lead to shifts of the core levels, although this effect is typically only a few tenths of an eV<sup>[25]</sup>, not the 1 eV observed for the 1+ component.

Objection to connecting the 1+ broadening with surface roughening can be based on the argument that this broadening is first observed following room temperature oxidation when the residual resistance is low. However, in the case of Ni(210), the presence of disordered overlayers containing a hint of facet structure at -140°C preceded the formation of the full faceted structure at 250°C.

Surface roughening also would cause another effect identifiable in the XPS spectra: increased inelastic scattering of escaping photoelectrons. Examination of the raw XPS data over a large energy range shows that the inelastic-electron background level is lowest (and equal) for the clean and the oxidized room temperature surfaces. The highest background was present for the warmed oxidized surface; in fact, that background level remained unchanged after the warmed samples cooled back down to room temperature, indicating that the effect is not simply due to a temperature dependence of the inelastic-electron loss mechanisms (however, firing

at 1400°C does restore the background to its pre-oxidation level). Such an XPS background increase is probably due to additional inelastic scattering of photoelectrons as they travel through the escape layer to the vacuum. The change in background upon warming is evident in the Figure 2 O 1s peak, low binding energy side, and is due to inelastic electrons from parent Nb 3d and 3p peaks at lower binding energy. Figure 2 Nb 3d is misleading about background level above 215 eV because plasmons present on the low kinetic energy (high binding energy) side of the Nb peak are not correctly modeled by the curve-fitting.

Further investigation of possible structure-related effects on these surfaces requires the use of LEED to determine if, indeed, faceting or another structural disruption occurs, provided the diffracting structures are oriented and of a lateral size larger than the diffraction coherence width (several tens of nm). Independent of those results, however, the present studies do show conclusively that low concentrations of oxygen can have detrimental effects on the performance of high purity Nb cavities.

#### Magnetic Field:

As is often the case, the results obtained with the 120 *mG* ambient magnetic field are difficult to understand. Since the effect is frequently reproducible only to within a factor of two, the only conclusion that can be made with any confidence is that the increase in residual resistance due to ambient magnetic field is several times larger on the cavities with warmed oxide layers than on the clean cavities. Thus, formation of fluxoid pinning centers is likely associated with the process responsible for the enhanced surface resistance.

## ACKNOWLEDGEMENT

The authors are indebted to Maury Tigner for many conversations and much encouragement, to Hasan Padamsee for many informative discussions and to David Gallagher for valuable discussions on chemical bonding in metal oxides.

## - REFERENCES

+ Present address: Department of Physics, University of Washington, Seattle, WA 98195.

- 1.] F. Palmer, IEEE Trans. Mag. MAG-23, 1617 (1987).
- 2.] E. L. Garwin, F. K. King, R. E. Kirby and O. Aita, J. Appl. Phys. 61, 1145 (1987).
- 3.] F. Palmer and M. Tigner, IEEE Trans. Mag. MAG-21, 1011 (1985).
- 4.] H. Farrell and M. Strongin, Surface Sci. 38, 18 (1973).
- 5.] S. Hofmann and J. M. Sanz, J. Trace and Microprobe Tech. 1, 213 (1983).
- 6.] R. E. Kirby, E. L. Garwin, F. K. King and A. R. Nyaiesh, J. Appl. Phys. 62, 1400 (1987).
- 7.] A. R. Nyaiesh, E. L. Garwin, F. K. King and R. E. Kirby, J. Vac. Sci. Technol. A4, 2356 (1986).
- 8.] P. Wilson, SLAC-TN-70-35 (Stanford Linear Accelerator Center, 1970).
- 9.] J. Turneure and I. Weissman, J. Appl. Phys. 39, 4417 (1968).
- 10.] J. Halbritter, Z. Physik 238, 466 (1970).
- 11.] P. Kneisel, R. Vincon, and J. Halbritter, Nuc. Inst. Meth. 188, 669 (1981).
- 12.] K. Schultze, J. of Met. May, 1981, p. 33.
- 13.] A. Abrikosov, L. Gorkov, R. Dzyaloshinski, Quantum Field Theoretical Methods in Statistical Physics, p. 315, (Pergamon Press, Oxford, 1965).

- 14.] M. Tinkam, Introduction to Superconductivity, p. 77 (R. E. Krieger Pub. Co., Huntington, N. Y., 1980).
- 15.] R. Powers and M. Doyle, J. Appl. Phys. 30, 514 (1959).
- 16.] J. Halbritter, Appl. Phys. A43, 1 (1987) and references therein.
- 17.] I. Lindau and W. E. Spicer, J. Appl. Phys. 45, 3720 (1974).
- 18.] R. A. Pollak, H. J. Stioz, S. I. Raider, and R. F. Marks, Oxidation of Metals 20, 185 (1983).
- 19.] A. Darlinski and J. Halbritter, Surf. Interface Anal. 10, 223 (1987).
- 20.] L. van Torne and G. Thomas, Acta Met. 12, 601 (1964).
- 21.] M. W. Roberts and C. S. McKee, Chemistry of the Metal-Gas Interface, (Oxford University Press, Oxford, 1978).
- 22.] T. W. Haas, A. G. Jackson, and M. P. Hooker, J. Chem. Phys. 46, 3025 (1967).
- 23.] R. E. Kirby, C. S. McKee and M. W. Roberts, Surface Sci. 55, 725 (1976).
- 24.] W. Gopel, Surface Sci. 139, 333 (1984).
- 25.] K. A. Bertness, J. J. Yeh, D. J. Friedman, P. H. Mahowald, A. K. Wahi, T. Kendelewicz, I. Lindau, and W. E. Spicer, Phys. Rev. B38, 5406 (1988).

## FIGURE CAPTIONS

- 1.] Temperature *vs.* time for Nb sample. Solid lines show when XPS data were collected.
- 2.] Curve-fitted XPS spectra taken while oxidized Nb was warmed from 24°C to 350°C. Different curves correspond to temperature ranges shown in Figure 1.
- 3.] BCS resistance at 2K (a), residual resistance (b), and enhancement of residual resistance due to a 120 *mG* field applied during cooldown (c) for an oxidized Nb cavity after warming in vacuum to the indicated temperature. Square points show values prior to oxidation. See text for explanation of solid line in (a).
- 4.] Calculated dependence of BCS resistance on purity of the Nb. Experimental data from Cornell are also shown.
- 5.] Oxygen concentration profiles calculated with the diffusion equation for Nb warmed to successively higher temperatures for 5 minutes at each indicated temperature.
- 6.] Curve-fitted XPS Nb 3d spectrum of Figure 2A. Component peaks contributing to total fit are: 1, 2 - fired (1400°C) Nb metal ( $\text{Nb}^0$ ); 3, 4 -  $\text{Nb}_2\text{O}_5$  ( $\text{Nb}^{5+}$ ); 5, 6 -  $\text{Nb}^{1+}$  (valence determined from binding energy shift relative to  $\text{Nb}^0$  peak).

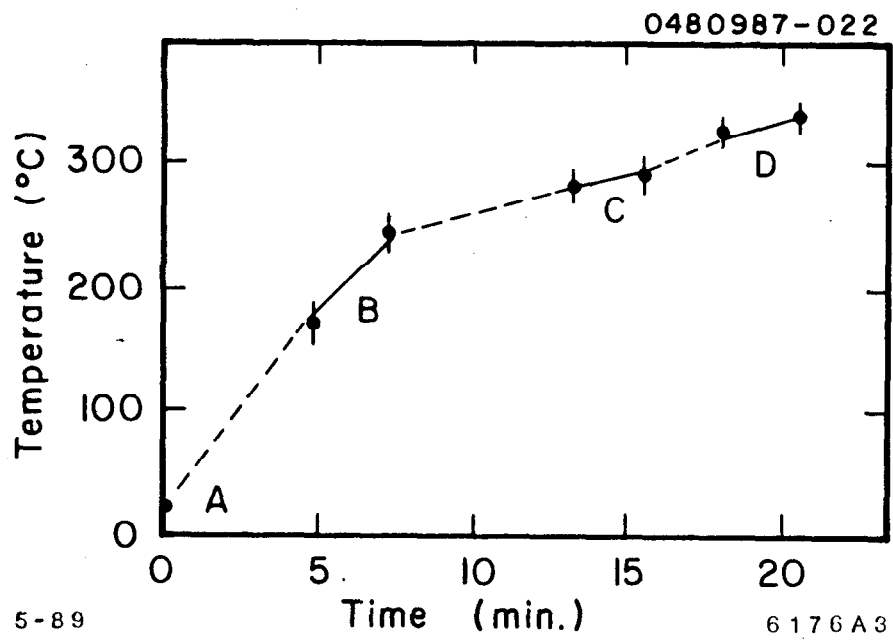


Fig. 1

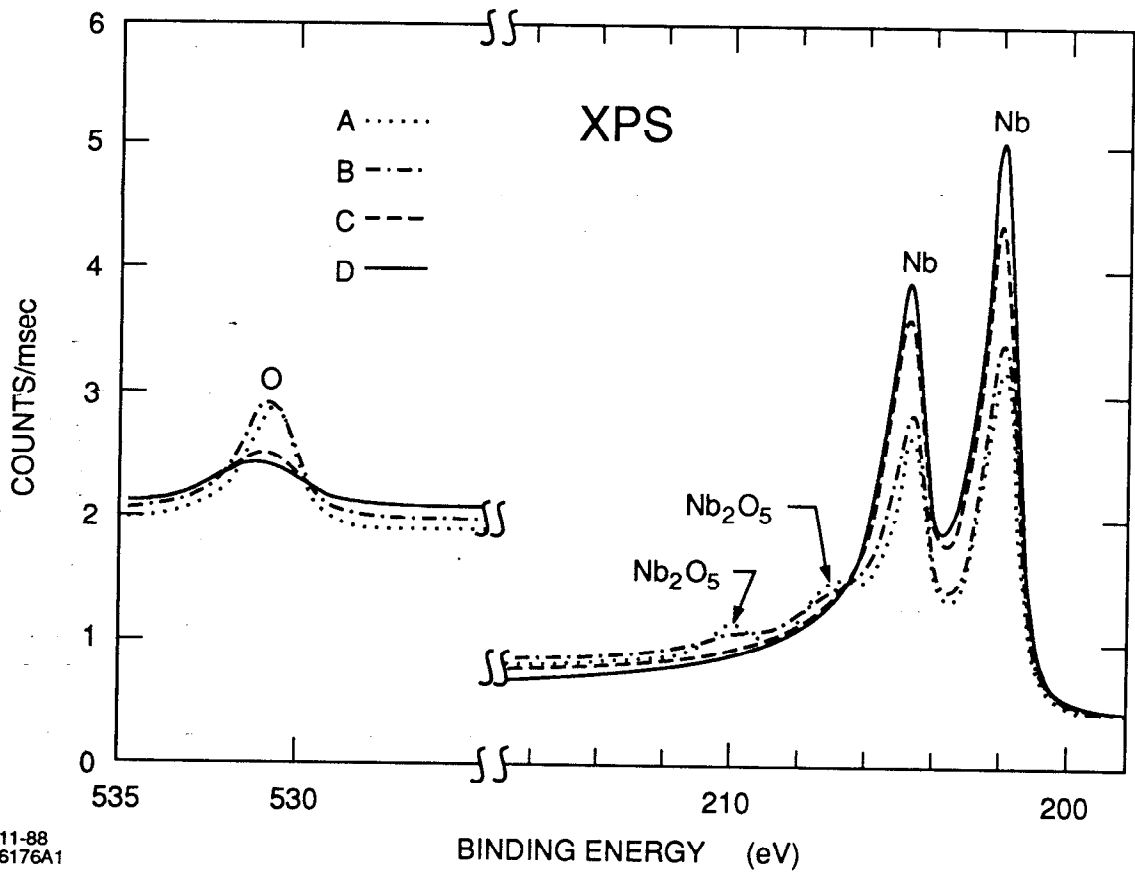


Fig. 2

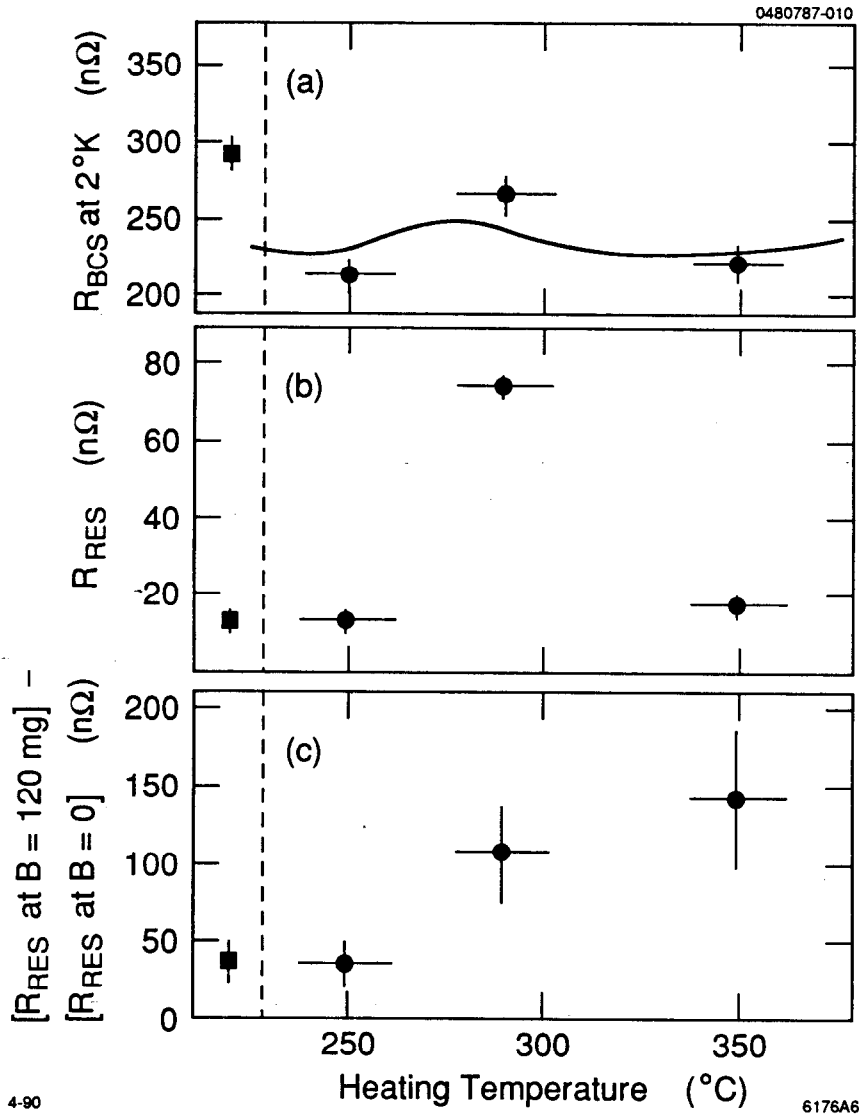


Fig. 3

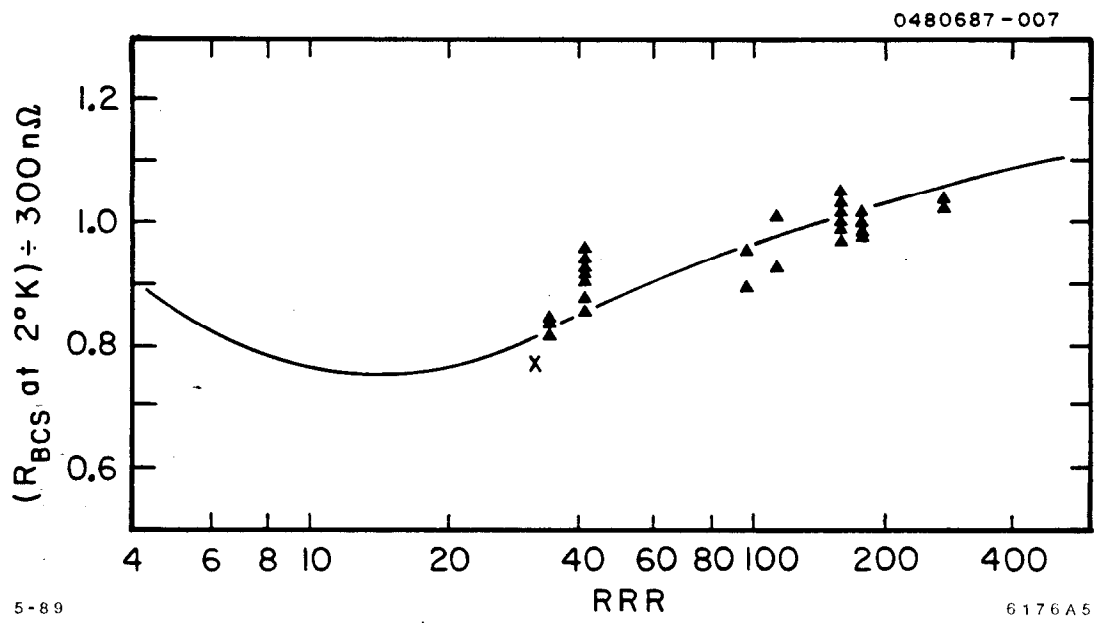


Fig. 4

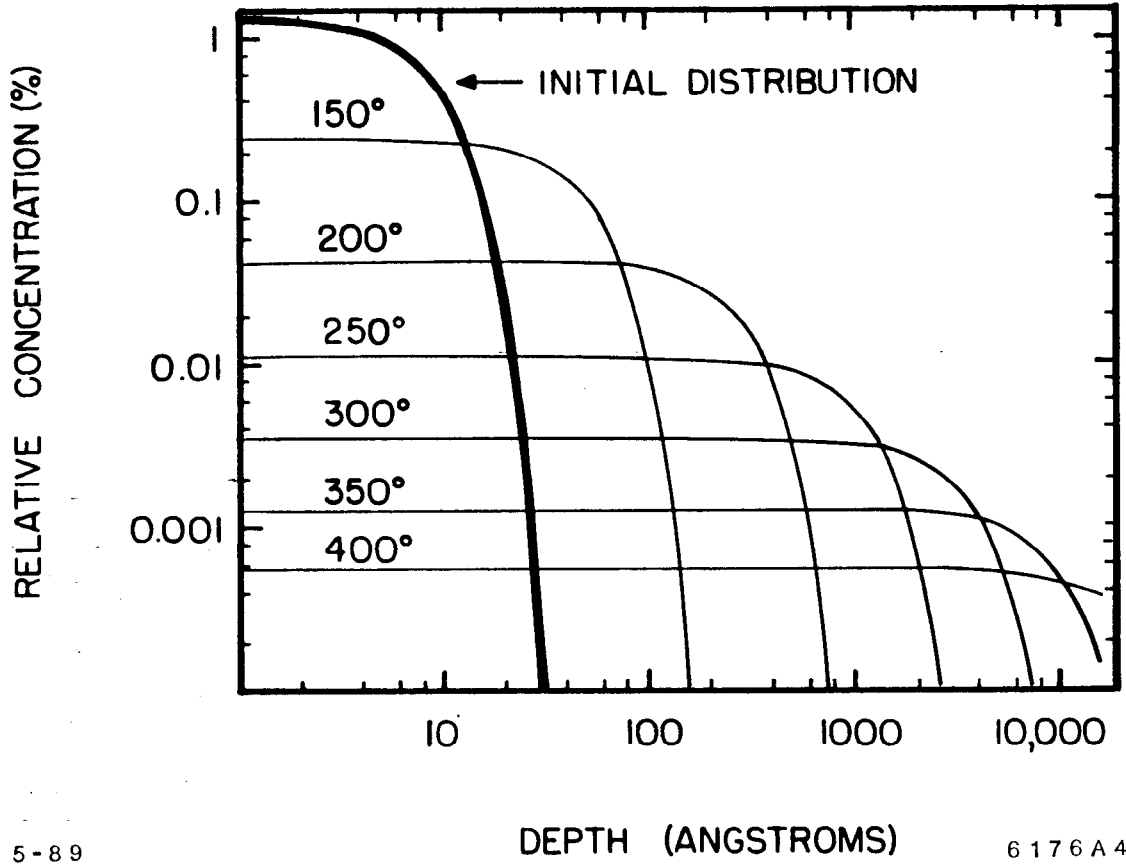


Fig. 5

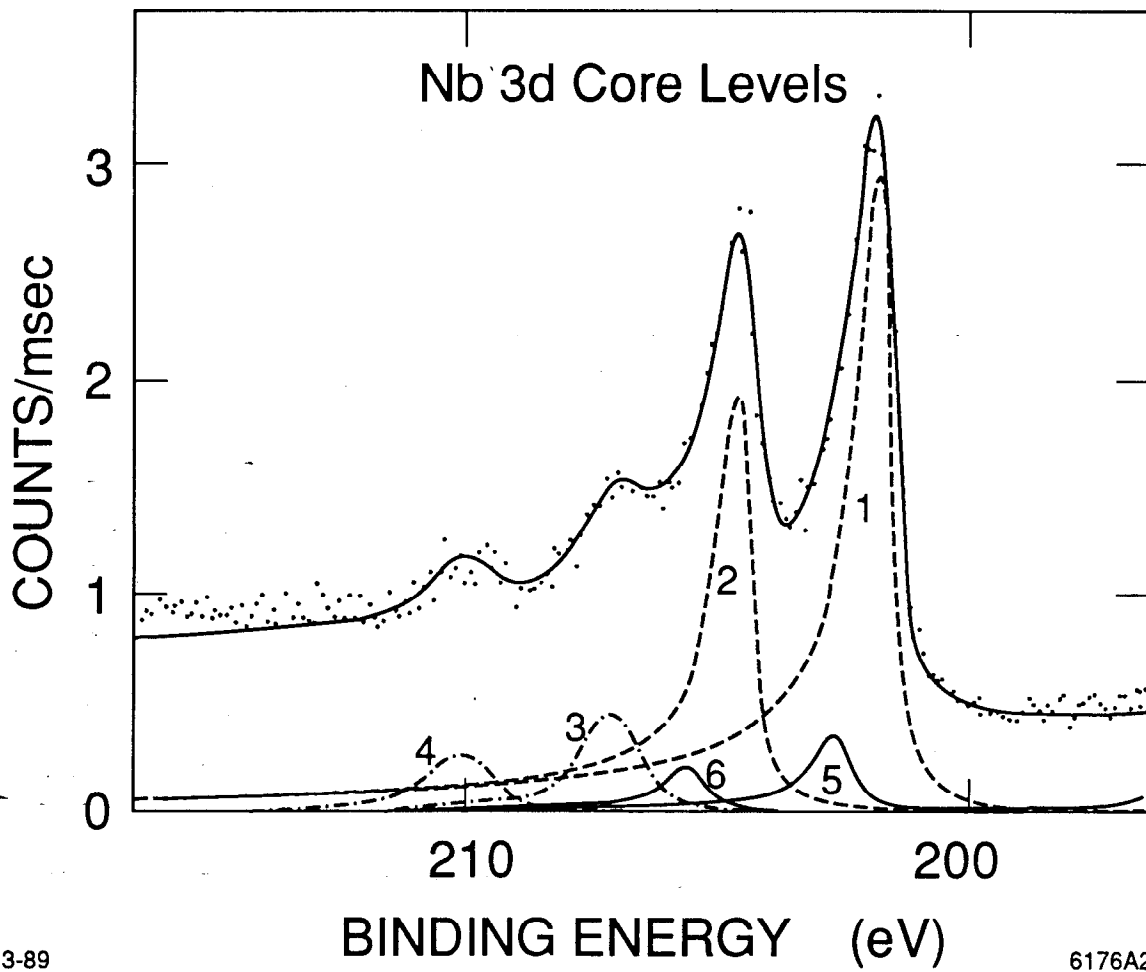


Fig. 6